Full Paper
doi.org/10.1002/chem.202001553

Nanoparticles |Hot Paper|

Solvent-Dependent Growth and Stabilization Mechanisms of Surfactant-Free Colloidal Pt Nanoparticles

Jonathan Quinson,*[a] Sarah Neumann+,[b] Laura Kacenauskaite+,[a] Jan Bucher,[c] Jacob J. K. Kirkensgaard,[d] Søren B. Simonsen,[e] Luise Theil Kuhn,[e] Alessandro Zana,[c] Tom Vosch,[a] Mehtap Oezaslan,[f, g] Sebastian Kunz,[b, h] and Matthias Arenz*[c]

Abstract: Understanding the formation of nanoparticles (NPs) is key to develop materials by sustainable routes. The Co4Cat™ process is a new synthesis of precious metal NPs in alkaline mono-alcohols well-suited to develop active nanocatalysts. The synthesis is 'facile', surfactant-free and performed under mild conditions like low temperature. The reducing properties of the solvent are here shown to strongly influence the formation of Pt NPs. Based on the in situ formation of CO adsorbed on the NP surface by solvent oxidation, a model is proposed that accounts for the different growth and stabilization mechanisms as well as re-dispersion properties of the surfactant-free NPs in different solvents. Using in situ and ex situ characterizations, it is established that in methanol, a slow nucleation with a limited NP growth is achieved. In ethanol, a fast nucleation followed by continuous and pronounced particle sintering occurs.

[a] Dr. J. Quinson, L. Kacenauskaite,+ Prof. Dr. T. Vosch
Department of Chemistry
University of Copenhagen
Universitetsparken 5, 2100 Copenhagen Ø (Denmark)
E-mail: jonathan.quinson@chem.ku.dk

[b] Dr. S. Neumann,+ Dr. S. Kunz
Institute for Applied and Physical Chemistry
University of Bremen
Leobenerstraße, 28359 Bremen (Germany)

[c] Dr. J. Bucher, A. Zana, Prof. Dr. M. Arenz
Department of Chemistry and Biochemistry
University of Bern
Freiestrasse 3, 3012 Bern (Switzerland)
E-mail: matthias.arenz@dcb.unibe.ch

[d] Prof. Dr. J. J. K. Kirkensgaard
Department of Food Science
University of Copenhagen
Rolighedsvej 26, 1958 Frederiksberg C (Denmark)

[e] Prof. Dr. S. B. Simonsen, Prof. Dr. L. Theil Kuhn
Imaging and Structural Analysis
Department of Energy Conversion and Storage
Technical University of Denmark
Fysikvej Bldg. 310, 2800 Kgs. Lyngby (Denmark)

[f] Prof. Dr. M. Oezaslan
Department of Chemistry, School of Mathematics and Science
Carl von Ossietzky University of Oldenburg
26111 Oldenburg (Germany)

[g] Prof. Dr. M. Oezaslan
Institute of Technical Chemistry
Technical University of Braunschweig
38106 Braunschweig (Germany)

[h] Dr. S. Kunz
Central Department Research, Development, Technological Services (CRDS)
Südzucker AG
Wormser Straße 11, 67283 Obrigheim (Germany)

[+] These authors contributed equally.

Supporting information and the ORCID identification number(s) for the author(s) of this article can be found under:
https://doi.org/10.1002/chem.202001553.

Introduction

Nanoparticles (NPs) find applications in an increasing number of technologies and are expected to contribute solving worldwide challenges in energy production and storage,[1] chemical production,[2] water remediation[3] or medicine,[4] to name only a few examples. To address specific needs, studying the growth mechanism of NPs is a rewarding strategy.[5,6] Understanding the formation of NPs usually leads to a controlled design of NPs with desirable features: for example, composition or functionalization to tune activity, stability[7] or selectivity[8] in catalysis. Fundamental research often focuses on wet-chemical syntheses to prepare NPs due to usually good scalability and reproducibility.[5,9] Typically, colloidal syntheses require surfactants or molecular additives to tune NP properties. Additives used to 'protect' the NPs are typically polymers, anions and/or viscous media.[10,11] These additives ensure simple size and/or shape control, favor colloidal stability and facilitate further processing by providing for instance suitable re-dispersion properties.[12]

Unfortunately, the additives typically need to be removed,[13] in particular for catalytic applications to obtain a 'free' catalytic surface. Their removal requires energy and time-consuming steps, with hazardous chemicals and/or harsh conditions. These steps can ultimately decrease reproducibility and negatively impact the catalytic properties. Moreover, additives are often derived from petroleum-based resources and are not environmentally friendly. For cheap, safe and green production processes, 'surfactant-free' approaches are receiving increasing attention from both academia and industries.[14] Last, understanding fully *why, when* or *how* additives influence the nucleation and growth of colloidal NPs remains a challenge.[15] Despite their multiple benefits for both fundamental research

and research-and-development, surfactant-free syntheses are still challenging to perform and control.

The Co4Cat™ process is a surfactant-free, one-step synthesis that requires only a metal precursor, a mono-alcohol, a base and energy (e.g. thermal treatment, microwaves or UV-light).[16] The NPs obtained by this method show superior catalytic activity compared to state-of-the-art catalysts for chemical production and energy conversion.[16,17] These improved properties can be attributed to the absence of surfactants, the improved dispersion at high metal loadings after supporting step on a support material, no need for extensive washing and no need for pre-treatment steps, resulting in readily active catalysts. Although often referred to as 'unprotected',[10,18] surfactant-free NPs must contain some form of surface functionalization that ensures stable colloidal dispersions. To optimize this synthesis approach, extend it to other materials and ultimately use it as a reference platform to study and understand more broadly the effect of additives in colloidal syntheses, a deeper understanding of surfactant-free NP formation and stabilization is first required.

In the present work, it is shown that the Co4Cat™ synthesis is an ideal platform to investigate parameters otherwise challenging to probe in colloidal syntheses. The price for the relative simplicity of this 'mono-alcohol' synthesis, that is, the absence of any surfactants, low temperature, low pressure, no need for inert atmosphere etc., is indeed sensitivity to parameters that are usually 'disregarded' because they are not expected to strongly influence size or colloidal properties in state-of-the-art colloidal approaches using surfactants.[19] One of the most important parameters in colloidal syntheses is obviously the solvent. We investigate the influence of the solvent properties on the surfactant-free particle formation and stabilization. Platinum (Pt) is chosen as case study since it is an important catalytic element for energy, automotive, chemical synthesis but also medicine and solvent remediation.[3,4,7,20] Using transmission electron microscopy (TEM), X-ray absorption near edge structure spectroscopy (XANES), in situ small angle X-ray scattering (SAXS), Fourier-transform infra-red spectroscopy (FTIR), micro Raman spectroscopy, head-space gas chromatography coupled to mass spectrometry (GC-MS), UV–vis absorption and fluorescence measurements, it is established why the formation mechanisms of Pt NPs strongly differ in the two simplest 'green' mono-alcohols:[21] methanol and ethanol.

Results and Discussion

General synthesis and use of 'aged' precursors

In alkaline methanol, it takes ca. 15 minutes in a microwave reactor synthesis before a color change is observed from yellow to dark brown for 2.5 mM H_2PtCl_6 solution (total volume of 80 mL), see Figure 1a. This color change is indicative of the formation of *fcc* Pt NPs as previously reported.[16] In the alkaline methanol-based synthesis, the reaction time, that is, the time required for the formation of particles indicated by a color change from yellow to black, corresponds to the consecutive reduction of Pt^{IV} to Pt^{II} and eventually Pt^0. This reaction time

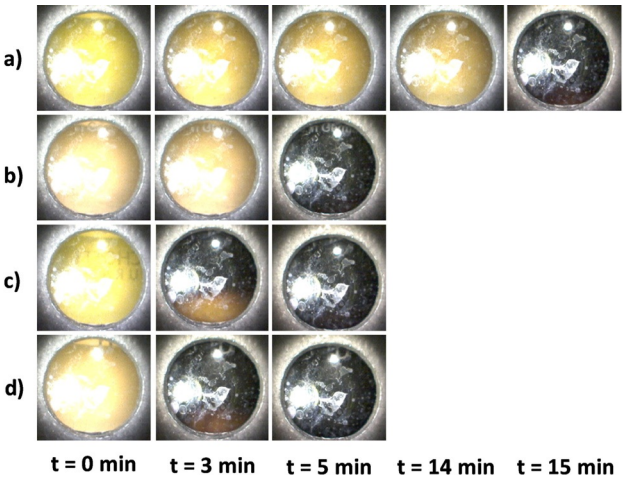

Figure 1. Pictures of 2.5 mM H_2PtCl_6 in alkaline (a, b) methanol and (c,d) ethanol for different times of continuous microwave heating. The reaction mixtures were obtained with (a,c) a freshly prepared precursor, (b,d) with a precursor irradiated 30 minutes with UV light prior to mixing with the alkaline solvent.

can be significantly shortened when the precursor is dissolved in methanol and not immediately used for the synthesis, but stored as a stock solution prior to application for NP synthesis.[22] Such 'aged' precursor solutions are obtained by storing a 20 mM H_2PtCl_6 solution (without base) while remaining exposed to ambient day light and room temperature for a week ('time-aged'). 'Aged' solutions can also be obtained in a faster manner by irradiating 20 mM H_2PtCl_6 solution with UV lamps for 30 minutes ('UV-aged'). These 'aged' precursor solutions contain an increased proportion of Pt^{II} species, as previously demonstrated in methanol by UV–vis absorption and X-ray absorption spectroscopy measurements.[22,23] During the ageing process the reduction of the Pt^{IV} complex occurs in parallel to the oxidation of the solvent to formic acid and methyl carbonate.[22] Due to the higher proportion of Pt^{II} species, the nucleation is ca. 5 times faster if an 'aged' precursor is used for the synthesis in alkaline conditions, see Figure 1a,b.

In addition to previous work on 'aged' precursors in methanol,[22] here we report an additional characterization, see Figure 2. Using Raman spectroscopy, changes are observed when a fresh solution of H_2PtCl_6 turns into a 'time-aged' solution. The typical two peaks at 319 and 342 cm^{-1} ascribed to Pt-Cl bounds in $[PtCl_6]^{2-}$,[24] turn into one broad feature, with a maximum peak at around 330 cm^{-1} in methanol attributed to $[PtCl_4]^{2-}$ species, see Figure S**1**.

In alkaline ethanol, upon microwave heating, a color change occurs in less than 5 minutes when a freshly prepared H_2PtCl_6 precursor is used, see Figure 1c. Using Raman spectroscopy, it is observed that a fresh H_2PtCl_6 solution in ethanol features the same two peaks at 318 and 342 cm^{-1} as for methanol. Upon ageing, these two peaks become a single peak as well, which is centered at 340 cm^{-1}. 'Time-aged' solutions of Pt^{IV} precursor in ethanol are characterized by a decrease in the intensity of the UV–vis absorption peak at 268 nm, indicative of the disappearance of the initial $[Pt^{IV}Cl_6]^{2-}$ complex, see Figure 3 and Fig-

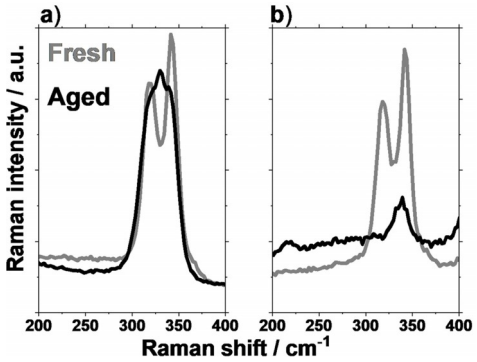

Figure 2. Raman spectra of fresh (grey) and time-aged (black) 50 mM H_2PtCl_6 solutions in (a) methanol and (b) ethanol (no base).

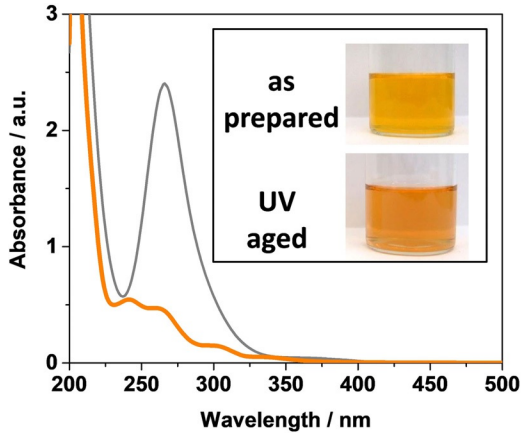

Figure 3. UV–vis absorption spectra of H_2PtCl_6 in ethanol. The grey line corresponds to the fresh solution. The orange bold line corresponds to a UV-aged solution (30 minutes irradiation with UV lamps). The inset is a collection of pictures showing the solution of 20 mM H_2PtCl_6 in ethanol: fresh (top) and UV-aged (bottom).

ure S2. In parallel, an increase in the proportion of Pt^{II} species in the 'time-aged' precursor in ethanol is confirmed by XANES data, see Table 1. It is therefore concluded that in both methanol and ethanol the initial $H_2Pt^{IV}Cl_6$ complex undergoes a reduction to Pt^{II} upon ageing.

Comparing the effect of using 'aged' precursor in methanol and ethanol on the kinetics of formation of the Pt NPs, it is found that in a microwave reactor this effect is less pronounced in alkaline ethanol because the reaction time is significantly shorter as compared to alkaline methanol, independent of whether using 'fresh' or 'aged' H_2PtCl_6 solutions as precursor, see Figure 1 c,d. In parallel, an increase in the proportion of Pt^{II} species in the 'aged' precursor in ethanol is confirmed by XANES data, see Table 1. This means, that the reaction time is reduced to ca. 2–3 minutes independent of whether the precursors used for the synthesis contains mainly Pt^{II} or Pt^{IV} species in alkaline ethanol.

Kinetics of the Pt NP formation

It could be argued that the differences in kinetics observed in Figure 1 relate to the fact that ethanol is a better solvent to absorb microwaves. The energy dissipation factor tan(δ) indicates how well a solvent absorb microwaves. The higher tan(δ), the more suitable the solvent is for synthesis (strong absorber). For ethanol this factor is slightly higher than for methanol (0.6 vs. 0.3).[25] However, even when performed thermally without microwave and at lower temperature, the reaction of the complex still occurs faster in alkaline ethanol. This faster formation of Pt NPs cannot be explained only by the reducing properties of the solvent since methanol should be a better reducing agent than ethanol.[26] To perform detailed kinetics studies, the Pt NP formation conveniently can be induced in closed vessels, using a water (alternatively oil) bath approach, allowing to slow down the reaction kinetics which facilitates the study of the precursor conversion to Pt NPs. Using this approach, it is observed that similar to the microwave synthesis, the formation of Pt NPs is still faster in ethanol than in methanol, see Figure S3.

The Pt L_3 edge XANES measurements confirm the fast conversion of Pt^{IV} to Pt^{II}, and further to Pt^0, in alkaline ethanol, see Table 2 and S1. Using a water bath at 70 °C, it takes only 45 minutes to nearly fully convert all the Pt^{IV} to Pt^0 in alkaline ethanol, whereas after ca. 2 hours only 42 wt. % of the Pt is converted to Pt^0 in alkaline methanol. These results confirm the faster reaction time in alkaline ethanol. It also indicates that once Pt^{II} species are formed they quickly get reduced to Pt^0 in alkaline ethanol.

Raman spectroscopy was used to follow the initial steps of the reaction in alkaline conditions, see Figure 4. In alkaline methanol, the peaks at 319 and 343 cm^{-1} remain unchanged, with or without heating to up to 65 °C. By comparison, in ethanol the fresh H_2PtCl_6 precursor solution undergoes rapid changes. As soon as the alkaline ethanol is added to the fresh

Table 1. Pt L_3 edge XANES data for H_2PtCl_6 solutions in ethanol: fresh and UV-aged.

Solvent	Ethanol	
Treatment	Fresh	UV-aged
Pt^{IV} [wt. %]	95.5 ± 0.6	15.9 ± 1.8
Pt^{II} [wt. %]	4.5 ± 2.4	84.1 ± 1.1
Pt^0 [wt. %]	0	0
white line intensity	2.11	1.58
ΔE_0 [eV]	−0.222 ± 0.008	0.030 ± 0.022
R	0.001	0.003

Table 2. Results from Pt L_3 edge XANES data for the synthesis of colloidal Pt NP dispersions using the Co4Cat process in alkaline methanol and ethanol after various reaction times (see Experimental Section for further details on the synthesis, Table S1 and Figure S4).

Alkaline solvent	Time	Pt^{IV} [wt. %]	Pt^{II} [wt. %]	Pt^0 [wt.%]
	0h00	100	–	–
methanol	0h30	100.0 ± 0.0	0.0 ± 1.7	–
	1h55	8.1 ± 3.8	50.2 ± 2.8	41.7 ± 1.6
	0h00	100	–	–
ethanol	0h30	63.0 ± 1.9	–	37.0 ± 2.6
	0h45	7.1 ± 6.7	–	92.9 ± 0.3

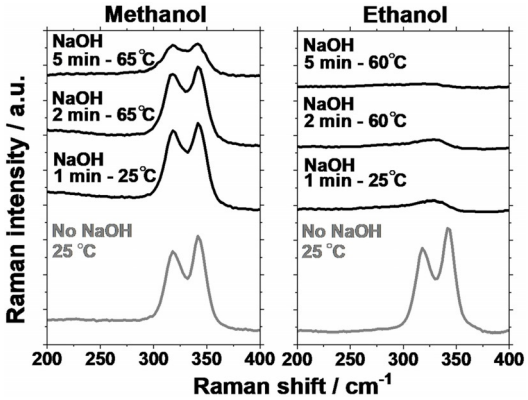

Figure 4. Raman spectra of fresh H_2PtCl_6 precursor solutions in methanol and ethanol, without and with addition of NaOH, as indicated. Time and temperature from the start of the experiment are indicated (note that this time is not the time after addition of NaOH to the fresh H_2PtCl_6 precursor solution but the time after heating up and exposure to laser light).

precursor, the strong peaks at 319 and 343 cm^{-1} disappear and are replaced by a smaller peak at 327 cm^{-1} which completely disappears upon heating the solution to a temperature of 60 °C. The bands related to the solvent also decreased significantly which indicates the formation of Pt NPs absorbing the light from the laser beam. This is confirmed by observing a strong and almost immediate decrease in intensity of the Raman band related to the solvent in ethanol and a slower decrease in the case of methanol. The faster formation of NPs (Pt^0) in the Raman experiment is in agreement with the XANES data. These differences in kinetics for the particle formation in alkaline ethanol and methanol point towards a strong influence of the chemical properties of the solvent on the formation mechanisms. In particular it seems that Pt^{IV} species as well as Pt^{II} species are more quickly reduced to Pt^0 in alkaline ethanol, see Figure 2, Figure 4 and Table 2. To further clarify the influence of different alkaline solvents in the stabilization and reaction of Pt^{IV} or Pt^{II} complexes the solvent-related side reactions were analyzed.

Solvent-related side reactions in alkaline media

To assess possible by-products of the solvent formed during the NP synthesis and their possible influence on the nucleation and particle growth process, UV–vis absorption and fluorescence measurements were performed, Figure 5. In this comparative study, ethylene glycol (EG) was also considered since it is a common solvent to perform the synthesis of 'unprotected' NPs[10,18,27,28] and the formation mechanism of NPs in EG is still subject to investigation.[18,29,30]

Stock solutions of alkaline solvents (stored at room temperature and exposed to light for one month) were subjected to a microwave induced heat treatment identical to those performed during NP synthesis but without any H_2PtCl_6 precursor (this is why the conditions for the EG synthesis are significantly different:160 °C for 3 minutes).

The solutions were first studied by UV–vis absorption spectroscopy, see Figure 5 a–c. The'time-aged' alkaline stock solutions do not show any features as compared to a background recorded with the pure solvent. However, upon heating the alkaline EG and alkaline ethanol exhibit new features in the region 240–420 nm. By comparison, alkaline methanol exhibits no significant difference before or after the heat treatment. This demonstrates that at the temperature at which the synthesis is typically performed, alkaline EG and ethanol undergo modifications—even without the reaction partner H_2PtCl_6—whereas alkaline methanol is 'stable'. The color change typically observed under highly alkaline conditions in EG and ethanol after extended period of storage supports further this hypothesis, see Figure S**5**. This color change is attributed in ethanol to the degradation of the solvent.[31] Characterization by fluorescence measurements, see Figure 5 d, indicates that fluorescent species are formed in minor contents. This observation is compatible with the presence of side reactions suggested from the UV–vis absorption measurements.

In methanol, neither additional UV–vis adsorption peaks nor fluorescent species were observed after heat treatment of alkaline solutions. No color change is observed for alkaline methanol either, even at high NaOH concentration and after storage for several months, see Figure S**5**. In a very simplistic view, within the limits of the characterization performed here, this indicates that the degradation of methanol in alkaline conditions is not favored.

The fact that alkaline ethanol undergoes more side-reactions in alkaline media than methanol, see Figure 5, might influence the particle formation as well as the further processing in supporting the NPs, but the later needs further investigation.

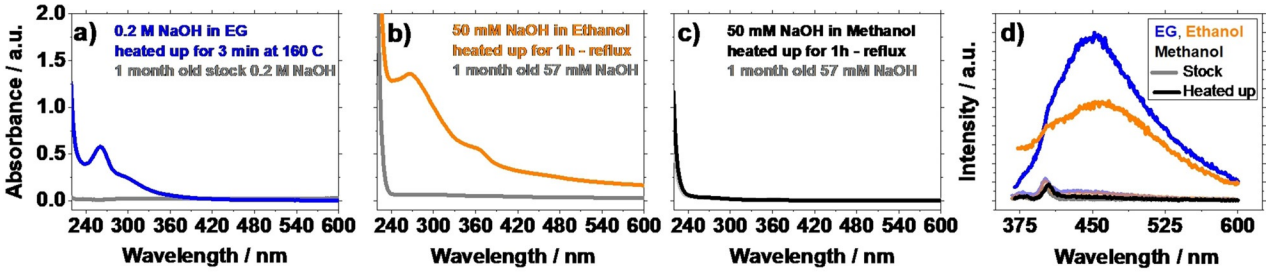

Figure 5. (a-c) UV–vis absorption spectra of 1-month old stock solutions of NaOH in different solvents and heat-treated solution of the same alkaline solutions with (a) EG, (b) ethanol and (c) methanol as solvents. (d) Fluorescence spectra (excitation wavelength: 360 nm) of NaOH solutions of EG (blue), ethanol (orange) and methanol (black) before (lighter lines) and after (darker lines) microwave-reactor heating. No H_2PtCl_6 was used. Peaks around 400 mn in (d) correspond to Raman scattering from the solvent.

From a mechanistic point of view, it has been proposed based on TEM images that the fluorescent species formed in EG could be carbon dots and could favor the formation of NPs.[30,32] Since the UV–vis absorption or fluorescence signals from such 'side-products' are not detected in methanol (without attempt here to establish the exact nature of the fluorescence species) the presented results do not support the hypothesis that carbon dots are needed for NP nucleation.

Growth and stability of the Pt NPs

The growth and stabilization of the Pt NPs in the different alkaline solvents has been investigated with zeta potential measurements. For the zeta potential of Pt NPs prepared in methanol -43.0 ± 0.6 mV was determined, whereas the NPs prepared in ethanol have a Zeta potential of -13 ± 1.9 mV, see also Figure S**6**. This indicates that negatively charged species like chloride or hydroxyl anions account at least partially for the NP stabilization, in agreement with previous reports.[19,22] The lower value for the NPs prepared in methanol suggests a higher stability of NPs in this solvent.[33] This is in good agreement with relative stability observed by eye of colloidal dispersions obtained in these two solvents.

In the following section, we investigated if the different formation kinetics and stabilization of Pt NPs observed in the two solvents influence the obtained particle size. An exclusive focus is given on the growth of the NPs after nucleation: that is, from a point where size estimation of Pt NPs is possible by TEM or SAXS (ca. >1 nm in diameter).

In a first approach, TEM was used to evaluate the size of the formed NPs, see Figure 6. The synthesis was performed with 8 mL of 2.5 mM H_2PtCl_6 in alkaline ethanol in a microwave reactor and the reaction was stopped at different times: (a) 1 minute, (b) 5 minutes, (c) 15 minutes and (d) 1 hour. The average diameter of the nanostructures obtained is (a) 1.9 ± 0.7 nm, (b) 2.0 ± 0.6 nm, (c) 2.3 ± 2.0 nm and (d) 3.5 ± 1.6 nm, respectively. These results show that in alkaline ethanol, the size of the Pt NPs increases with time of synthesis. Due to the variety of shapes observed by TEM, the larger size is likely to be a result from NP sintering. Interestingly, the increase in particle size can be influenced with the gas atmosphere during the reaction. Typically, the synthesis is performed without purging the solvent with a gas. However, in a CO atmosphere, the obtained particle size is limited (e) to 1.6 ± 0.4 nm even after 1 hour of synthesis.

In alkaline methanol (without CO atmosphere) no synthesis time dependent particle size is observed. The obtained particle size is always around 2 nm, even after 1 hour of synthesis (f) the size is still 1.9 ± 0.6 nm.

The same trends are observed if alkaline solutions of H_2PtCl_6 precursor are left for several hours at 70 °C in a hot water bath in closed containers. Aliquots characterized for different synthesis time are shown in Figure S**3**. In methanol the size is rather consistent around 2 nm over time. In ethanol the size of the NP size increases with time from ca 1.5 nm to larger agglomerates of few hundreds of nanometers after several hours of heating.

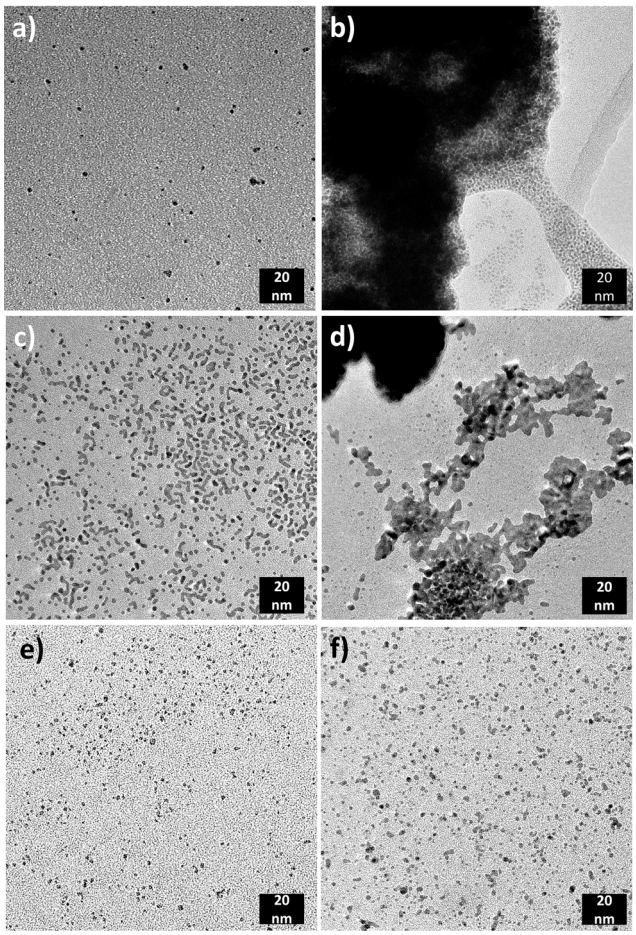

Figure 6. TEM images of Pt NPs obtained by the Co4Cat mono-alcohol process in (a–d) alkaline ethanol, (e) alkaline ethanol under CO atmosphere, (f) alkaline methanol. See text for experimental details.

While TEM measurements allow characterizing the NPs size at different points in time, in situ SAXS experiments were performed to gain real-time information on the dynamic increase in size of the Pt NPs, see Figure 7. In alkaline methanol the size of the Pt NPs changes as follows: after a period where no size fit could realistically be performed due to very low signal-to-background ratio (grey area, see also Figure S7–8, Table S2) a constant size around 2 nm is quickly reached, see Figure 7a. The time evolution of the NP diameter and the size range observed are in agreement with a relative fast nucleation and moderate growth previously reported.[16,22]

By comparison in alkaline ethanol, a much shorter period for particle formation is observed. At the start, the signal-to-background ratio is still low and leads to fits with very small or very large size deviation. The signal-to-background ratio progressively increases over time which accounts for the trend to observe the mean value of the diameter increasing with the reaction time. Upon reaching a size of ca. 1 nm, the signal-to-background ratio is sufficient for proper fitting and it is observed that the NP size continuously increases, see Figure 7b. In conclusion, the nucleation process is slower in alkaline methanol and followed by a moderate growth of NPs reaching a diameter of ca. 2 nm over time. In contrast, the nucleation is faster in

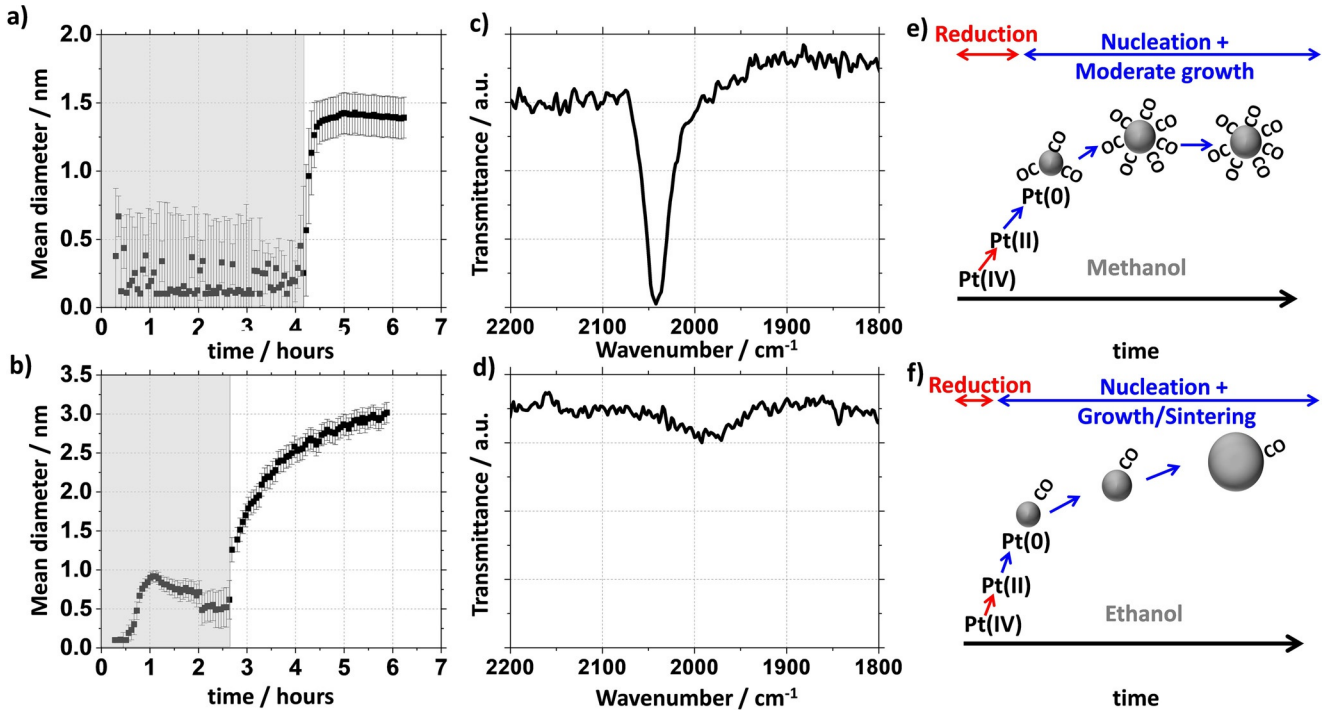

Figure 7. Evolution of the size of Pt NPs followed in situ by SAXS in alkaline (a) methanol and (b) ethanol. The grey area corresponds to data point where no reliable fit could be performed due to low signal-to-background ratio. See also Figures S7–8. FTIR spectra for Pt NPs obtained in alkaline (c) methanol (d) ethanol. Schematic representation of the formation mechanism of Pt NPs in alkaline (e) methanol and (f) ethanol.

alkaline ethanol, but the particle size continuously increases over time in agreement with the TEM results.

FTIR was used to correlate these results to the surface functionalization of Pt NPs of ca. 2 nm obtained in alkaline methanol or ethanol. In particular the band related to CO adsorbed (CO_{ad}) on the NP surface was studied as it is proposed to be an important stabilizing molecule and its presence in the synthesis influences the obtained particle size (see above). In Figure 7c,d FTIR spectra of Pt NPs obtained in alkaline methanol and ethanol are displayed. The NPs synthesized in methanol exhibit a characteristic absorption peak around 2040 cm^{-1} corresponding to CO_{ad} on the Pt surface. This feature is typical of so-called 'unprotected' NPs as previously reported using EG as solvent.[18] In this respect, the qualification of 'unprotected'[18] NPs used in the literature is misleading as it is shown that the NPs are covered with residual functional groups like CO_{ad} and/or OH. Interestingly, the NPs synthesized in alkaline ethanol exhibit a much smaller signal for CO_{ad} pointing to a lower surface coverage. It however appears at a different wavenumber, which suggests that the surface coverage or the chemical identity of the NPs obtained by these two syntheses is not identical.

CO as stabilizing agent has been previously reported. The resulting CO protection was induced using CO atmosphere at room condition in solvents like toluene or tetrahydrofuran using synthesized in house bis- or tris- (dibenzylideneacetone)Pt complexes[34] or dimethylcyclooctadiene platinum complex.[35] Yet the CO stabilization was reported to not be enough to stabilize NPs and the use of polymers was preferred.[34] In synthesis performed in ethylene glycol from K_2PtCl_4 and H_2PtCl_6 in presence of acetate[35] or under alkaline conditions[18,36] the solvent is also reacting to lead to CO protection.[18,36,37] A similar CO protection is here achieved in methanol without the need for lethal CO gas atmosphere or high boiling point solvents.

In parallel to the formation of the NPs in methanol, oxidation products like CO_2 and methyl formate are detected by head-space GC-MS, see Figure 8. Their formation can be explained by the reduction of H_2PtCl_6 in alkaline media while the oxidation of methanol occurs. These products are not observed if Pt NPs obtained from a commercial supplier are heated up under reflux conditions in alkaline methanol, see Table S**3**. This indicates that these are reaction products mainly related to the NP formation from H_2PtCl_6. In ethanol, no additional CO_2 (no relative increase of the peak intensity at 1.5 min compared to a control sample with just ethanol) was detected but acetaldehyde was. The same product is also detected during the ageing procedure of H_2PtCl_6 in ethanol. Previously reported intermediates of methanol or ethanol degradation studied under different conditions like formaldehyde (T_{bp} = −19 °C, thus difficult to detect in our post-synthesis study)[23] and methyl acetate, respectively, were not identified by head space GC-MS.

It is proposed here that the respective reducing properties of the solvent, playing also here the role of reducing agent,[26] can explain the observed differences in nucleation and growth/sintering of Pt NPs in alkaline methanol and alkaline ethanol. Methanol is more easily oxidized, for example, to CO and CO_2, than ethanol.[38] We suggest that due to its oxidation properties, methanol more easily leads to CO_{ad} surface groups

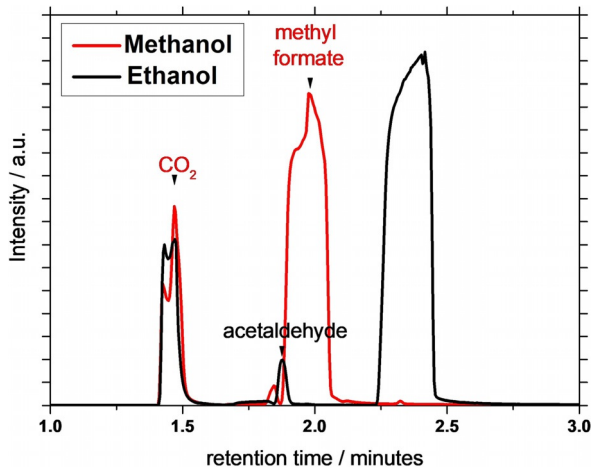

Figure 8. Head space GC-MS chromatograph of 2.5 mM H_2PtCl_6 in alkaline ethanol or methanol after microwave heating and Pt NP formation. The broad feature at 2 and 2.25 minutes correspond to methanol and ethanol, respectively. The first peak at 1.4 min corresponds to light gases like N_2 and CO. Methyl formate appears as an extra peak at 2.0 min on top of the methanol.

on the NP surface which prevents further growth. Less CO_{ad} surface groups are produced from the oxidation of ethanol, resulting in a particle sintering over time. Such model is in agreement with the size control observed in CO atmosphere and alkaline ethanol as well as head space GC-MS results where oxidation products and fragments of methanol are identified only in presence of H_2PtCl_6. Using alkaline methanol CO_{ad} surface groups are conveniently formed in situ stopping the particle growth whereas in alkaline ethanol the duration of the heating can be used to influence the NP size via particle sintering.

A simple model accounting for the different growth mechanisms in alkaline NaOH methanol and ethanol is summarized in Figure 7e,f. The likelihood of the solvent to reduce H_2PtCl_6 while being oxidized to CO, influences the mechanism. In EG the sintering of Pt NPs is also moderate.[39] It has been evidenced that EG can be cleaved homolytically to lead to CO_{ad}.[40] This simple model is therefore also in agreement with the formation mechanism of Pt NPs in alkaline EG.

Redispersion properties

The model also accounts for re-dispersion properties of Pt NPs. In Figure 9, focus is given on CO_{ad} bands for NPs re-dispersed in different solvents. NPs as-synthesized in ethanol do not show a pronounced CO_{ad} band, Figure 9a,b—black spectra. However, after re-dispersion in EG or methanol, a pronounced CO_{ad} band is formed, Figure 9a,b—grey spectra. NPs prepared in methanol show a CO_{ad} band as-synthesized but also after re-dispersion in EG, Figure 9c. Finally, if the NPs are synthesized in ethanol under CO atmosphere, a pronounced CO_{ad} band is observed as well, Figure 9d. NPs obtained in EG can progressively recover CO_{ad} coverage by degradation of EG at the Pt surface.[18,28] For NPs synthesized in methanol or ethanol, after re-dispersion in EG it is shown here that the CO_{ad} bands also become more pronounced over time.

The observed shift in position of the peak towards lower wavenumber may be attributed to several factors. The initial spectra (black) were recorded in alkaline conditions; re-dispersion (grey) was in pure solvent (without base). The change in NaOH concentration can influence the local environment of the CO_{ad} as well as its coverage thus inducing a shift in peak position.[41] After washing and re-dispersion in the new solvent it can take some time to establish equilibrium for CO_{ad} coverage. In addition, it was recently shown that traces of HCl, used here to collect and re-disperse the NPs, can lead to leaching of Pt atoms resulting in a change of NP size.[39] Smaller NPs present a CO_{ad} peak at lower wavenumber as well.[18]

The FTIR data support the ability of already formed Pt NPs to '(re)cover themselves' with CO_{ad} by solvent oxidation and thus stabilizing the suspension. The stability of the colloidal suspensions decreases in the relative order EG > methanol > ethanol. NPs synthesized in ethanol under CO atmosphere are also stable for several weeks. The improved stability in EG can be also at least partially related to the high viscosity of the solvent—as opposed to the low viscosity of methanol and ethanol. In addition, the relative colloidal stability correlates also well with the presence of a CO_{ad} band which stresses further the key role of CO_{ad} to stabilize 'unprotected' NPs.

Size control strategies

Based on the model proposed and summarized in Figure 7e,f, different strategies can be explored to achieve size control in the Co4Cat process. Using methanol a size of around 2 nm is obtained regardless of the time of synthesis.[16,22] The synthesis in methanol is robust to changes in experimental parameters. A first option to tune the size of the NPs is therefore to control the time of synthesis in alkaline ethanol. Alternatively, if the

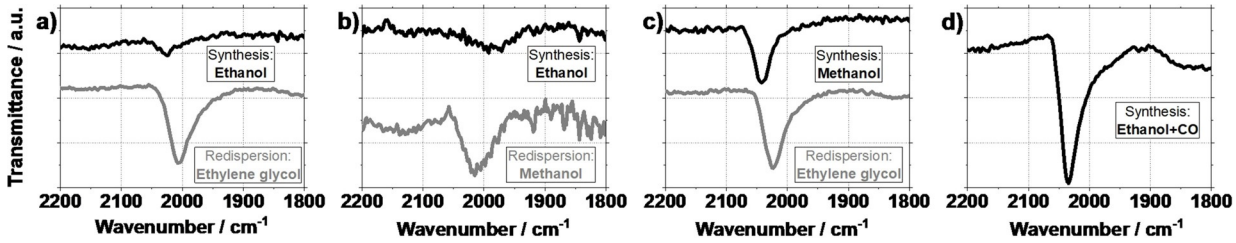

Figure 9. (a–c) FTIR spectra of NPs as-synthesized in alkaline solvent (black) and re-dispersed in different solvents after washing with HCl (grey). (d) FTIR spectrum of Pt NPs as-synthesized in alkaline ethanol under CO atmosphere.

amount of CO_{ad} formed is controlled, different NP sizes should be obtained. This can be achieved using CO (lethal) gas, but methanol can fulfil the role as CO source as well, in a safer way by '*in situ*' formation.

To achieve a larger particle size, the amount of methanol should be minimized in mixtures between methanol and a solvent with poor oxidation properties. Larger NPs are indeed formed in methanol-water mixtures as the water content increases.[16,22] In methanol-ethanol mixtures with different ratios of the two solvents and different synthesis times the size can be controlled as well, see Table S**4** and Figure S**9**. For high methanol content, the time of synthesis has little influence on size and stability of the NPs.

For higher ethanol content, the size of the NPs increases more markedly with time of experiment and NP sedimentation is more pronounced. This result supports our proposed stabilization model.

In ethanol, adding water also leads to larger NPs, see Figure 10. For example, in a water bath synthesis (70–75 °C) for 8 mL solutions of 2.5 mM H_2PtCl_6 with (a) 0%, (b) 25%, (c) 50% and (d) 75% water (vol.%), the solutions turned darker in (a) 15, (b) 45, (c) 60 and (d) 135 minutes, respectively. Once the solutions turn dark the vessel was left for 1 hour to react and finally lead to NPs with sizes of (a) 1.6 ± 0.4 nm, (b) 1.7 ± 0.7 nm (c) 2.3 ± 1.1 nm and (d) 3.5 ± 0.8 nm. However, large agglomerates form at higher water content (e.g. 75% water). As the water content increases the colloidal stability is reduced and NPs tend to sediment, see Figure S**10**. Achieving size control adding water in ethanol and at the same time colloidal stability is therefore more challenging than with methanol.

An important last difference between ethanol and methanol is their behavior at low H_2PtCl_6 concentration. In methanol, there is no effect of the water content on size of the NPs at low H_2PtCl_6 concentration.[16,22] In ethanol, even at relatively low concentration of H_2PtCl_6 precursor (e.g. 0.5 mM), the influence of water is pronounced. To demonstrate this, synthesis was performed in a microwave reactor in 80 mL methanol with 0.5 mM H_2PtCl_6. The size obtained is little affected by the amount of water: 1.6 ± 0.5 nm without water (40 minutes synthesis) and 1.5 ± 0.5 nm with 80% water (40 minutes synthesis). By comparison the behavior in alkaline ethanol is shown in Figure 11. For 0.5 mM H_2PtCl_6 in alkaline ethanol without adding water the NPs are (a) 1.7 ± 0.4 nm (10 minutes synthesis corresponding to ca. 8 minutes under reflux conditions after the solution turned dark) and the size increases to (b) 2.0 ± 1.0 nm with 80% water (20 minutes synthesis, corresponding to ca. 3 minutes under reflux conditions after the solution turned dark). As the H_2PtCl_6 concentration increases to 2.5 mM the effect of water is more pronounced with (c) 1.4 ± 0.4 nm without water and (d) 2.7 ± 0.54 nm for the smallest individual NPs that can be observed with 80% water. This means that in contrast to methanol, size control is achieved at low H_2PtCl_6 concentration by adding water in alkaline ethanol.

These results suggest that to obtain stable colloidal dispersions of Pt NPs in alkaline ethanol a low H_2PtCl_6 concentration is preferable. At lower H_2PtCl_6 concentrations the amount of CO_{ad} produced is enough to protect few NPs as opposed to high H_2PtCl_6 concentrations where with respect to the number of NPs 'less' CO is formed. As a consequence, at lower H_2PtCl_6 concentration (e.g. 0.5 mM) no strong influence of the reaction time could be observed in ethanol, just like in methanol. The NPs obtained using alkaline ethanol can be produced with a small size of ca. 1–2 nm, see Figure 11, and give stable colloidal dispersion, see Figure 12. This is the size typically obtained in EG synthesis[27] or methanol[16] and is considered ideal for a range of applications[7] in homo/hetero catalysis as well as electrocatalysis and possibly in medicine.

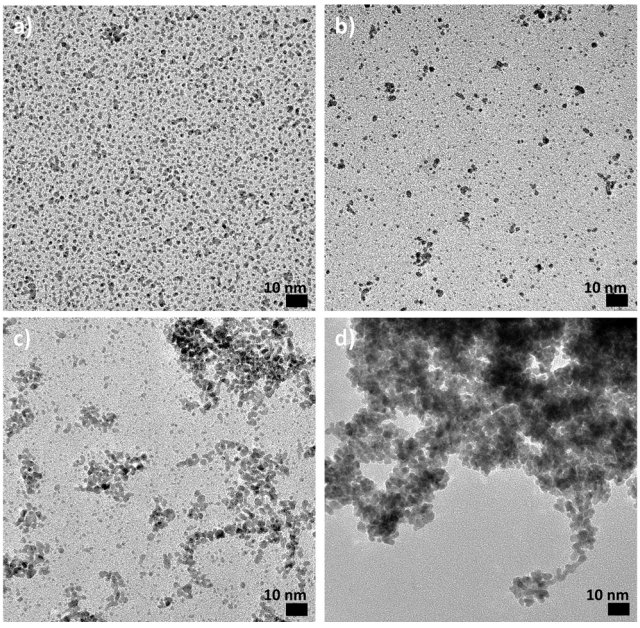

Figure 10. TEM images of Pt NPs obtained using 2.5 mM H_2PtCl_6 in alkaline NaOH ethanol when (a) 0%, (b) 25%, (c) 50% and (d) 75% water is added to ethanol.

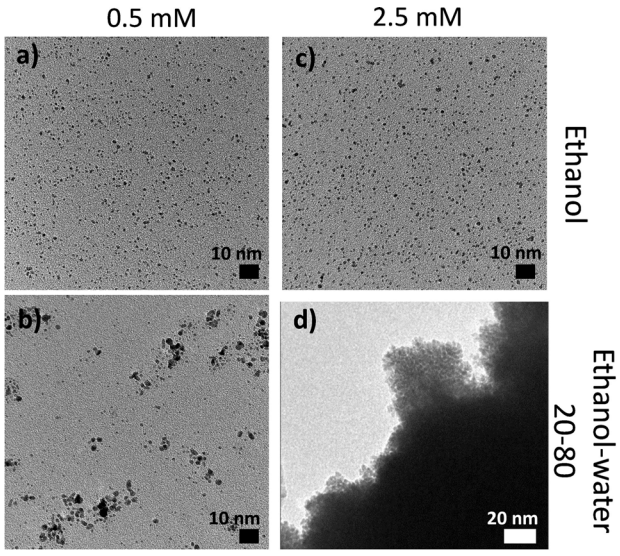

Figure 11. TEM images of the Pt NPs obtained for (a,b) 10 minutes and (c,d) 20 minutes synthesis using 80 mL of (a,b) alkaline NaOH ethanol as solvent or (c,d) 80% water in alkaline NaOH ethanol. The H_2PtCl_6 concentration was (a,c) 0.5 mM and (b,d) 2.5 mM.

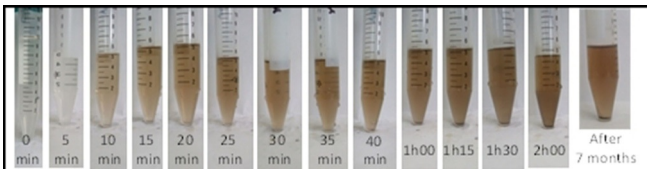

Figure 12. Images at different times of 4 mL of 0.5 mM H_2PtCl_6 in alkaline (NaOH) ethanol after the solution is simply left in a closed plastic or glass container placed in a hot water bath at 70 °C. The last image was taken 7 months after the synthesis was performed.

Fundamental, practical and industrial considerations

The selection between methanol and ethanol depends on practical factors. Alkaline methanol appears as a 'less complex' solvent, respective to the UV–vis absorption and fluorescence measurements performed here. It is more suited if a ca. 2 nm fixed particle size should be obtained in the most reproducible fashion. For industrial applications, ethanol can be obtained at large scale by sustainable routes and is arguably a cheaper, 'greener', and safer chemical than methanol. However, the solubility of NaOH in ethanol is slightly lower than in methanol, yet high enough to perform the synthesis of precious metal NPs. Methanol has a lower boiling point than ethanol ($T_{bp\text{-}methanol} = 65\,^{\circ}C < T_{bp\text{-}ethanol} = 78\,^{\circ}C$), NP synthesis and further processing like solvent removal for NPs collection or solvent recycling can then be performed at lower temperature so at lower energy cost in methanol.

Conclusions

It is demonstrated that methanol and ethanol are suitable 'green' solvents[21] to produce NPs by the surfactant-free Co4Cat™ process. The NPs form by nucleation and growth, followed by a sintering over time in the absence of CO_{ad} protective groups. The formation of CO_{ad} is determined by the reducing properties of the solvent. Thus, in methanol a fixed NP sized control is achieved in a reproducible way with almost no sintering over extensive heating times. This finding is related to the facile oxidation of methanol to CO_{ad} leading to protective groups impairing NP sintering. By control of the amount of formed CO_{ad} the obtained NP size can be varied. Selecting suitable solvent mixtures thereby is a sustainable and safer approach than using a CO reaction atmosphere.

The findings reported have direct relevance for fundamental studies. The knowledge gained on the synthesis method presented, is a strong starting point and platform to gain deeper insights into the role of surfactants in NP formation, for example, in studies where the surfactant-free Co4Cat™ synthesis is used as a 'control' colloidal synthesis. The results are also directly relevant to design further synthesis strategies to propose reliable and large-scale production route of surfactant-free NPs.

Experimental Section

Chemicals: All chemicals were used as received: $H_2PtCl_6{\cdot}6H_2O$ (99.9%, Alfa Aesar); K_2PtCl_6 (99.9%, Alfa Aesar); K_2PtCl_4 (99.9% Alfa Aesar); NaOH (98%, Alfa Aesar or >99%); methanol (≥99.8%, Sigma–Aldrich); ethanol (99.9%, Kemetyl); ethylene glycol (EG, 99+%, Sigma–Aldrich); water (Milli-Q, Millipore, resistivity >18.2 MΩ·cm, total organic carbon (TOC) <5 ppb); HCl (30% Suprapur®, EMD Millipore, Merck KGaA), commercial 46.5 wt% Pt/C catalyst (TEC10E50E, Tanaka Kikinzoku Kogyo).

Synthesis of Pt NPs in mono-alcohols: H_2PtCl_6 is dissolved in alkaline (NaOH) methanol or ethanol, or their mixture thereof with water, with the concentrations of H_2PtCl_6, NaOH, as well as the total volume and time of synthesis indicated in the text. Unless otherwise specified, all experiments were performed with a NaOH/Pt molar ratio of 20. The nucleation of Pt NPs can be initiated by thermal treatment: using a hot-water bath or a microwave reactor. The respective method is indicated in the text.

Hot water bath synthesis: A hot water bath heated to 70–75 °C and stirred with a magnetic stirrer (1000 rotations per minute, rpm) was used. H_2PtCl_6 dissolved in an alkaline (NaOH) methanol or ethanol solution (also stirred with a magnetic stirrer at 1000 rpm) was placed in a closed glass or plastic container (typical volume of 8 mL). The container was then placed in the hot water bath. The reaction times are indicated in the text.

Microwave synthesis: H_2PtCl_6 dissolved in an alkaline (NaOH) methanol or ethanol was irradiated with a constant power of 100 W using a microwave reactor (CEM Discover SP) in a reflux set-up for a synthesis time as indicated in the text. While the solution was irradiated, a flow of N_2 was passed on the outside of the vessel to cool it down, otherwise the temperature raised too quickly. No stirring was performed.

Ageing of precursor: To artificially age the solutions of H_2PtCl_6, the solutions were exposed for 30 minutes to the light of ten standard UV mercury lamps (PL-L-24W/10/4P Hg, Philips) for 'UV-aged' precursors. Alternatively, the solutions were left at room temperature and exposed to daylight for at least a week for 'time-aged' precursors. Unless otherwise specified, daily freshly prepared solutions were used in all syntheses.

Re-dispersion studies: For re-dispersion studies, the as-synthesized NPs with a starting concentration of 2.5 mM H_2PtCl_6 to give a concentration of ca. 0.5 $mg_{Pt}\,mL^{-1}$ were precipitated and collected by mixing with aqueous solutions of 1 M HCl as typically performed for the polyol synthesis.[28,42] After centrifugation (5 to 10 minutes at 4000 rotations per minute, 2400 relative centrifugal force in a Sigma 2–5 laboratory centrifuge, Sigma) the NPs were re-dispersed at the same concentration in various solvents as indicated.

X-ray absorption near edge structure spectroscopy (XANES): X-ray absorption spectroscopy measurements were carried out at the B18 beamline of Diamond Light Source (DLS), UK (beam current of 300 mA, storage ring energy of 3.0 GeV) or at the SuperXAS beamline of Swiss Light Source (SLS), Switzerland (beam current of 400 mA, storage ring energy of 2.4 GeV). At the B18 beamline, the Pt L_3 edge XAS spectra were recorded in fluorescence mode by using a 9 element Ge solid state detector system, while the acquisition of the Pt L_3 edge XAS spectra was performed in transmission mode at the SuperXAS beamline by using N_2-filled ionization chambers with lengths of 15 and 30 cm for the incident (I_0) and transmitted (I_1 and I_2) X-ray intensities. The averaged spectra were analyzed by using the IFEFFIT software suite.[43] All spectra were background subtracted and normalized. The energy units (eV) were converted to photoelectron wave vector k units ($Å^{-1}$) by as-

signing the photoelectron energy origin, E_0, corresponding to $k=0$, to the first inflection point of the absorption edge.

Linear combination fit (LCF) method was carried out to establish the oxidation state of Pt species in the colloidal dispersions by using the respective XANES reference spectra of K_2PtCl_4, K_2PtCl_6 and Pt foil. From the XANES data, a LCF analysis was used to evaluate the relative weight percentage of Pt^0, Pt^{II} and Pt^{IV} and the related parameters: white line intensity, shift of energy (ΔE_0) at the corresponding edge and R factor (closeness of the fit as quality parameter) are reported.

To monitor the conversion of H_2PtCl_6 to Pt^0 a sealed container (total reaction volume of 16 mL) with 4 mM H_2PtCl_6 and a NaOH/Pt molar ratio of 20 was placed in a hot water bath at 70 °C under stirring. Aliquots of the reaction solution were sampled at different times and quenched by using liquid nitrogen prior to measurements performed at room temperature. In methanol a colour change to brown was observed at ca. 1 h 45 minutes during the experiments. In ethanol this colour change occurred after ca. 20 minutes.

Determination of particle size distributions by transmission electron microscopy (TEM): For the TEM analysis, a JEOL 2100 transmission electron microscope operated at 200 kV was used. Particle size and morphology were estimated by recording images at different magnifications (at least x300 000, x400 000, x500 000) in minimum three randomly selected areas. The samples were prepared for TEM analysis by dropping the dispersions containing the Pt NPs in low boiling point solvent (e.g. methanol, ethanol) on carbon coated copper TEM grids (Quantifoil). The particle size and size distribution analysis was performed by measuring the size (projected diameter) of at least 50 and more typically between 700–1000 Pt NPs using the software ImageJ. The mean diameter and the standard deviation (σ, in nm) for each sample are reported. For time dependent studies, aliquots of the reactive media were taken at desired times and deposited on TEM grids.

Determination of particle size distributions by small-angle X-ray scattering (SAXS): The size of the particles obtained was assessed by SAXS measurements as previously reported[27,44] Experiments were performed using a SAXSLab instrument (JJ-XRay) with a Rigaku 100 XL+ micro focus sealed X-ray tube and a Dectris 2D 300 K Pilatus detector installed at the Niels Bohr Institute of the University of Copenhagen. For in situ measurements: 10 mM $H_2PtCl_6.6H_2O$ and 200 mM NaOH in methanol or ethanol solutions were used to fill a quartz capillary placed itself in a temperature controlled holder. The same trends could be observed for 5 mM $H_2PtCl_6.6H_2O$ and 10 mM NaOH but the signal to noise ratios were improved at higher $H_2PtCl_6{\cdot}6H_2O$ and NaOH concentrations. The recording of the SAXS data started at room temperature and the temperature was then raised to 70 °C at ca. 7 °C min^{-1}.

The data analysis was performed using a method described previously[18,27] using a polydisperse spheres model. The first dataset recorded at room temperature was used as background. No major changes were observed if background using alkaline methanol or ethanol at room temperature or 70 °C was used. Each dataset was recorded for 3 minutes and the total time of experiments was between 2 and 10 hours. Control experiments show that performing the reaction at 50 °C requires longer time to observe a formation of NPs. At room temperature no NPs could be formed even after 10 hours of exposure to X-rays. The time dependence reported for the diameter of the NP was observed in at least four independent experiments for alkaline methanol and at least four independent experiments for alkaline ethanol.

Fast Fourier-Transform Infra-red (FTIR) measurements: The as-prepared Pt NPs in alkaline (NaOH) methanol, ethanol or re-dispersed in methanol, ethanol or EG were dropped onto a ZnSe crystal for attenuated total reflectance acquisition. As reference the same solution as the solvent in which the NPs were re-dispersed (methanol, ethanol, EG with or without NaOH) was used. The IR spectra were recorded in ATR mode on a Thermo-Nicolet Avatar 370 FT-IR spectrometer. All spectra were recorded with a resolution of 4 cm^{-1} and averaging 50 scans.

Head-space gas chromatography—mass spectrometry (GC-MS): A gas chromatograph (Agilent 6890 N Network GC System) with a headspace sampler (Agilent G1888 Network Headspace Sampler), with an Agilent 19091S-433 non-polar column (HP-5 ms (5%-phenyl) methyl poly siloxane, 30.0 m, 250 μm, 0.25 μm) connected to a mass spectrometer (Agilent 5973 inert Mass Selective Detector) was used. Chromatographs were acquired with a temperature ramp from 30 to 140 °C at 20 °C min^{-1}.

UV-vis absorption characterization: UV-vis absorption spectra were acquired with a Lambda1050 UV/VIS/NIR absorption spectrometer (PerkinElmer) by diluting the desired solution to a suitable concentration for spectroscopic measurements (typically 0.1 mM) and using the same solvent as for the measurements (e.g. methanol, ethanol or EG) for background.

Micro Raman spectroscopy: Raman measurements were performed using a micro-Raman setup in backscattering geometry. The 632.8 nm line of a HeNe laser (Thorlabs HRR170-1) was used (6.6 mW on top of the objective). The beam was focused in an inverted confocal microscope (Olympus IX71) by an Olympus CPlanFL N 10x objective inside the capillary tube containing the sample. Raman spectra were collected using a Princeton Instruments SPEC 10:100 B/LN-eXcelon CCD detector and an SP 2356 spectrometer with 600 g mm^{-1} grating. A LL01-633 filter (Semrock) was used to clean the laser light, a LPD02-633RU (Semrock) was used as dichroic mirror and 2 LP02-633RE filters (Semrock) were used to block the remaining laser light in the detection path. X-axis calibration was performed with a neon spectral lamp (6032 Newport). The acquisition time was 1 minute for each spectrum. No Y-axis corrections or background removal procedures were performed. Only a constant value was added or subtracted for display purposes.

For recording spectra, 50 mM H2PtCl6 in 1 M NaOH in methanol or ethanol were placed in sealed borocapillaries (Mark-Rohrchen, 1 mm outer diameter, 10 μm thick, 8 cm long) and heated up with a heat gun. Using a 632.8 nm laser no significant laser-induced reaction could be noticed. In most cases however the formation of Pt NPs lead to a complete attenuation of the signal, typically marked by the decrease in intensity of the peaks related to the solvent[45] despite the capillary still containing solvent. For kinetics study the first minute was recorded at room temperature (ca. 25 °C) and the later spectra while heating up.

Fluorescence measurements. A Cary Eclipse fluorescence spectrophotometer (Agilent Technologies) was used with methanol/ ethanol/ EG as a background. In all cases the samples were diluted to a suitable concentration for spectroscopic measurements (typically 0.1 mM). An excitation wavelength of 360 nm was used.

Zeta potential measurements: The analysis was carried out with a Litesizer 500 (Anton Paar) and the corresponding Software Kalliope. The cuvettes used were disposables (Sarstedt) with a path length of 10 mm equipped with a Univette (Anton Paar). Microwave synthesized Pt NPs from 2.5 mM H_2PtCl_6 alkaline solutions in methanol and ethanol, were diluted with methanol and ethanol, respectively in a ratio of 1:10 (final concentration of Pt for the analysis:

0.25 mM). The analysis temperature was adjusted to 20 °C. Further adjustments in the software were an equilibration time of 1 minute, a Hueckle approximation and a number of runs of 100. The solvent properties used were for methanol a refractive index of 1.3292, viscosity of 0.000594 Pa s and a relative permittivity of 30.57. For ethanol the refractive index used was 1.3571, a viscosity of 0.001144 Pa s and a relative permittivity of 24.3. A series of 5 measurements was carried out and an average value out of these 5 measurements was calculated.

Acknowledgements

B. J. Davies is thanked for her help with the GC-MS protocols. We would like to thank Prof. Bo Wegge Laursen, Prof. Thomas Just Sørensen and Prof. Matthew Johnson for the use of equipment. M.A. acknowledges the support from the Villum Foundation in form of a block stipend. J.Q. acknowledges the European Union's Horizon 2020 research and innovation program under the Marie Skłodowska-Curie grant agreement No 703366 (SELECTRON). J.Q. and J.J.K.K. acknowledge local support and continued access to the University of Copenhagen SAXSLab facility. Diamond Light Source, Hartwell, UK is thanked- in particular Dr. Giannantonio Cibin and Ann-Kathrin Geiger—for access to synchrotron beamline B18 (proposal SP12746). The Swiss Light Source (SLS) at the Paul Scherrer Institute, Switzerland is thanked—in particular Dr. Maarten Nachtegaal and Dr. Olga Safonava—for access to synchrotron beamline SuperXAS (proposal 20161303).

Conflict of interest

The authors declare that the general synthesis presented is subject to a patenting process (EP 3 329990 A1, WO 2018/099958 A1).

Keywords: Co4Cat technology · colloids · nanoparticles · surfactant-free · synthesis

[1] S. Basri, S. K. Kamarudin, W. R. W. Daud, Z. Yaakub, *Int. J. Hydrogen Energy* **2010**, *35*, 7957 – 7970.
[2] Y. Wang, J. L. Zhang, X. D. Wang, J. W. Ren, B. J. Zuo, Y. Q. Tang, *Top. Catal.* **2005**, *35*, 35 – 41.
[3] T. Pradeep, Anshup, *Thin Solid Films* **2009**, *517*, 6441 – 6478.
[4] M. Rai, A. P. Ingle, S. Birla, A. Yadav, C. A. Dos Santos, *Crit. Rev. Microbiol.* **2016**, *42*, 696 – 719.
[5] H. Zheng, R. K. Smith, Y.-w. Jun, C. Kisielowski, U. Dahmen, A. P. Alivisatos, *Science* **2009**, *324*, 1309 – 1312.
[6] a) J. Ren, R. D. Tilley, *J. Am. Chem. Soc.* **2007**, *129*, 3287 – 3291; b) S. Cheong, J. Watt, B. Ingham, M. F. Toney, R. D. Tilley, *J. Am. Chem. Soc.* **2009**, *131*, 14590 – 14595.
[7] E. Antolini, *Appl. Catal. B* **2016**, *181*, 298 – 313.
[8] I. Schrader, S. Neumann, R. Himstedt, A. Zana, J. Warneke, S. Kunz, *Chem. Commun.* **2015**, *51*, 16221 – 16224.
[9] a) N. Varghese, C. N. R. Rao, *J. Colloid Interface Sci.* **2012**, *365*, 117 – 121; b) M. Harada, N. Tamura, M. Takenaka, *J. Phys. Chem. C* **2011**, *115*, 14081 – 14092; c) M. Oezaslan, F. Hasche, P. Strasser, *Chem. Mater.* **2011**, *23*, 2159 – 2165.
[10] Y. Wang, J. W. Ren, K. Deng, L. L. Gui, Y. Q. Tang, *Chem. Mater.* **2000**, *12*, 1622 – 1627.
[11] a) C. W. Chen, D. Tano, M. Akashi, *J. Colloid Interface Sci.* **2000**, *225*, 349 – 358; b) J. Cookson, *Platinum Met. Rev.* **2012**, *56*, 83 – 98; c) Y. Y. Zheng, Z. J. Dou, Y. X. Fang, M. W. Li, X. Wu, J. H. Zeng, Z. H. Hou, S. J. Liao, *J. Power Sources* **2016**, *306*, 448 – 453.
[12] P. Losch, W. X. Huang, E. D. Goodman, C. J. Wrasman, A. Holm, A. R. Riscoe, J. A. Schwalbe, M. Cargnello, *Nano Today* **2019**, *24*, 15 – 47.
[13] a) M. Cargnello, C. Chen, B. T. Diroll, V. V. T. Doan-Nguyen, R. J. Gorte, C. B. Murray, *J. Am. Chem. Soc.* **2015**, *137*, 6906 – 6911; b) N. Naresh, F. G. S. Wasim, B. P. Ladewig, M. Neergat, *J. Mater. Chem. A* **2013**, *1*, 8553 – 8559; c) Z. Q. Niu, Y. D. Li, *Chem. Mater.* **2014**, *26*, 72 – 83; d) M. A. Montiel, F. J. Vidal-Iglesias, V. Montiel, J. Solla-Gullon, *Curr. Opin. Electrochem.* **2017**, *1*, 34 – 39; e) I. A. Safo, C. Dosche, M. Ozaslan, *ChemPhysChem* **2019**, *20*, 3010 – 3023; f) I. A. Safo, M. Oezaslan, *Electrochim. Acta* **2017**, *241*, 544 – 552.
[14] a) H. H. Duan, D. S. Wang, Y. D. Li, *Chem. Soc. Rev.* **2015**, *44*, 5778 – 5792; S. Olveira, S. P. Forster, S. Seeger, *J. Nanotechnol.* **2014**, Article ID: 324089; b) Q. L. Zhu, N. Tsumori, Q. Xu, *J. Am. Chem. Soc.* **2015**, *137*, 11743 – 11748; c) P. D. Burton, T. J. Boyle, A. K. Datye, *J. Catal.* **2011**, *280*, 145 – 149; d) P. T. Witte, P. H. Berben, S. Boland, E. H. Boymans, D. Vogt, J. W. Geus, J. G. Donkervoort, *Top. Catal.* **2012**, *55*, 505 – 511; e) R. Sharma, Y. Wang, F. Li, J. Chamier, S. M. Andersen, *ACS Omega* **2019**, *4*, 15711 – 15720.
[15] S. Mozaffari, W. H. Li, C. Thompson, S. Ivanov, S. Seifert, B. Lee, L. Kovarik, A. M. Karim, *Nanoscale* **2017**, *9*, 13772 – 13785.
[16] J. Quinson, S. Neumann, T. Wannmacher, L. Kacenauskaite, M. Inaba, J. Bucher, F. Bizzotto, S. B. Simonsen, L. T. Kuhn, D. Bujak, A. Zana, M. Arenz, S. Kunz, *Ang. Chem. Int. Ed.* **2018**, *57*, 12338 – 12341; *Angew. Chem.* **2018**, *130*, 12518 – 12521.
[17] F. Bizzotto, J. Quinson, A. Zana, J. Kirkensgaard, A. Dworzak, M. Oezaslan, M. Arenz, *Catal. Sci. Technol.* **2019**, *9*, 6345 – 6356.
[18] I. Schrader, J. Warneke, S. Neumann, S. Grotheer, A. A. Swane, J. J. K. Kirkensgaard, M. Arenz, S. Kunz, *J. Phys. Chem. C* **2015**, *119*, 17655 – 17661.
[19] J. Quinson, J. Bucher, S. B. Simonsen, L. T. Kuhn, S. Kunz, M. Arenz, *ACS Sustainable Chem. Eng.* **2019**, *7*, 13680 – 13686.
[20] a) B. G. Pollet, S. S. Kocha, I. Staffell, *Curr. Opin. Electrochem.* **2019**, *16*, 90 – 95; b) J. Leong, M. C. Schulze, M. B. Strand, D. Maloney, S. L. Frisco, H. N. Dinh, B. Pivovar, R. M. Richards, *Appl. Organomet. Chem.* **2014**, *28*, 1 – 17.
[21] D. Prat, A. Wells, J. Hayler, H. Sneddon, C. R. McElroy, S. Abou-Shehada, P. J. Dunn, *Green Chem.* **2016**, *18*, 288 – 296.
[22] J. Quinson, L. Kacenauskaite, J. Bucher, S. B. Simonsen, L. T. Kuhn, M. Oezaslan, S. Kunz, M. Arenz, *ChemSusChem* **2019**, *12*, 1229 – 1239.
[23] M. Wojnicki, P. Kwolek, *J. Photochem. Photobiol* **2016**, *314*, 133 – 142.
[24] L. A. Woodward, J. A. Creighton, *Spectrochim. Acta* **1961**, *17*, 594 – 599.
[25] D. C. Campos, E. L. Dall'Oglio, P. T. de Sousa, L. G. Vasconcelos, C. A. Kuhnen, *Fuel* **2014**, *117*, 957 – 965.
[26] T. S. Rodrigues, M. Zhao, T. H. Yang, K. D. Gilroy, A. G. M. da Silva, P. H. C. Camargo, Y. N. Xia, *Chem. Eur. J.* **2018**, *24*, 16944 – 16963.
[27] J. Quinson, M. Inaba, S. Neumann, A. A. Swane, J. Bucher, S. B. Simonsen, L. T. Kuhn, J. J. K. Kirkensgaard, K. M. O. Jensen, M. Oezaslan, S. Kunz, M. Arenz, *ACS Catal.* **2018**, *8*, 6627 – 6635.
[28] S. Neumann, S. Grotheer, J. Tielke, I. Schrader, J. Quinson, A. Zana, M. Oezaslan, M. Arenz, S. Kunz, *J. Mater. Chem. A* **2017**, *5*, 6140 – 6145.
[29] a) F. Fiévet, S. Ammar-Merah, R. Brayner, F. Chau, M. Giraud, F. Mammeri, J. Peron, J.-Y. Piquemal, L. Sicard, G. Viau, *Chem. Soc. Rev.* **2018**, *47*, 5187 – 5233; b) J. Quinson, L. Kacenauskaite, T. L. Christiansen, T. Vosch, M. Arenz, K. M. O. Jensen, *ACS Omega* **2018**, *3*, 10351 – 10356.
[30] L. Kacenauskaite, J. Quinson, H. Schultz, J. J. K. Kirkensgaard, S. Kunz, T. Vosch, M. Arenz, *ChemNanoMat* **2017**, *3*, 89 – 93.
[31] M. L. Sauer, D. F. Ollis, *J. Catal.* **1996**, *158*, 570 – 582.
[32] X. H. Gao, Y. Z. Lu, R. Z. Zhang, S. J. He, J. Ju, M. M. Liu, L. Li, W. Chen, *J. Mater. Chem. C* **2015**, *3*, 2302 – 2309.
[33] J. D. Clogston, A. K. Patri, *Characterization of Nanoparticles Intended for Drug Delivery*; (Eds.: S. E McNeil), Springer: Methods in Molecular biology, **2011**, 697, Chapter 6, pp. 63 – 70.
[34] A. Rodriguez, C. Amiens, B. Chaudret, M. J. Casanove, P. Lecante, J. S. Bradley, *Chem. Mater.* **1996**, *8*, 1978 – 1986.
[35] V. Latour, A. Maisonnat, Y. Coppel, V. Colliere, P. Fau, B. Chaudret, *Chem. Commun.* **2010**, *46*, 2683 – 2685.
[36] E. A. Baranova, C. Bock, D. Ilin, D. Wang, B. MacDougall, *Surf. Sci.* **2006**, *600*, 3502 – 3511.
[37] S. Gomez, L. Erades, K. Philippot, B. Chaudret, V. Colliere, O. Balmes, J. O. Bovin, *Chem. Commun.* **2001**, 1474 – 1475.

[38] a) L. R. Merte, M. Ahmadi, F. Behafarid, L. K. Ono, E. Lira, J. Matos, L. Li, J. C. Yang, B. R. Cuenya, *ACS Catal.* **2013**, *3*, 1460 – 1468; b) A. Sapi, F. Liu, X. Cai, C. M. Thompson, H. Wang, K. An, J. M. Krier, G. A. Somorjai, *Nano Lett.* **2014**, *14*, 6727 – 6730; c) M. C. Figueiredo, A. Santasalo-Aarnio, F. J. Vidal-Iglesias, J. Solla-Gullon, J. M. Feliu, K. Kontturi, T. Kallio, *Appl. Catal. B* **2013**, *140*, 378 – 385.
[39] S. Neumann, J. Schroder, F. Bizzotto, M. Arenz, A. Dworzak, M. Oezaslan, M. Baumer, S. Kunz, *ChemNanoMat* **2019**, *5*, 462 – 471.
[40] C. Bock, C. Paquet, M. Couillard, G. A. Botton, B. R. MacDougall, *J. Am. Chem. Soc.* **2004**, *126*, 8028 – 8037.
[41] C. W. Olsen, R. I. Masel, *Surf. Sci.* **1988**, *201*, 444 – 460.
[42] M. Inaba, J. Quinson, J. R. Bucher, M. Arenz, *J. Vis. Exp* **2018**, *133*, e57105.
[43] M. Newville, *J. Synchrotron Radiat.* **2001**, *8*, 322 – 324.
[44] a) J. Speder, L. Altmann, M. Roefzaad, M. Baumer, J. J. K. Kirkensgaard, K. Mortensen, M. Arenz, *Phys. Chem. Chem. Phys.* **2013**, *15*, 3602 – 3608; b) J. Speder, L. Altmann, M. Baumer, J. J. K. Kirkensgaard, K. Mortensen, M. Arenz, *RSC Adv.* **2014**, *4*, 14971 – 14978.
[45] Z. K. Meng, S. N. Cheng, G. I. Petrov, J. A. Jo, V. V. Yakovlev, *Advanced Biomedical and Clinical Diagnostic Systems XI* **2013**, Proceedings 8572, 85721G, https://doi.org/10.1117/12.2002923.

Manuscript received: March 31, 2020
Revised manuscript received: May 5, 2020
Accepted manuscript online: May 19, 2020
Version of record online: July 1, 2020